Robust SAMs of Ru(II) and Os(II) Polypyridines on Gold Surfaces: Exploring New Potentials

Frances A. Murphy[a], Stéphane Suárez[a], Egbert Figgemeier[b], Emma R. Schofield[a], Sylvia M. Draper[a,]*

[a] Chemistry Department, Sami Nasr Institute of Advanced Materials (SNIAM), Trinity College Dublin, College Green, Dublin 2, Ireland; [b] Department of Chemistry, University of Basel, Spitalstrasse 51, 4056 Basel, Switzerland.

smdraper@tcd.ie

RECEIVED DATE

ABSTRACT:

Metal complexes $[M(phtpy)(pztpy)](PF_6)_2$ (phtpy = 4'-phenyl-2,2':6',2''-terpyridine, pztpy = 4'-(*N*-piperazinyl)-2,2':6',2''-terpyridine, M = Ru, Os) were prepared and examined spectroscopically and electrochemically. The piperazine attachment was found to significantly modify the photophysical and electrochemical properties compared to the parent bis-terpyridine complexes, causing a red-shift of the ^{1}MLCT (23 nm) and a substantial cathodic shift of the redox potential (0.30 V for Ru, 0.23 V for Os). Self-assembled monolayers (SAMs) of the complexes on polished gold electrodes were generated simply *via* the *in situ* formation of a dithiocarbamate (DTC) anchoring group at the terminal piperazinyl nitrogen on the pztpy ligand. Cyclic voltammetry revealed that the monolayers show excellent reversible behaviour and exceptional stability. The high stability of the SAMs is attributed to the strong bidentate attachment to the gold surface of the DTC tether and the favourable low oxidation potentials of the complexes which result from the electron-rich piperazine nitrogen on the pztpy ligand. Such DTC-based SAMs demonstrate a substantial improvement over commonly-employed thiol-based systems, and offer new scope for future development.

Introduction

Self-assembled monolayers (SAMs) are monomolecular layers which are spontaneously formed by the adsorption of molecular constituents in a regular array on a substrate. The most well-established and understood are generated from the assembly of alkanethiols on gold surfaces. Applications of

alkanethiol monolayers on gold include the immobilisation of different photo-, chemical or electroactive groups for sensors[1] and biosensors,[2,3] optical data storage[4] and catalysis.[5] Gold electrodes are a particularly attractive platform for SAMs because cyclic voltammetry can be used to examine both monolayer structure and the kinetic parameters of long-range electron transfer of the resulting redox-active SAM.[6,7]

Of the known redox-active monolayers, those functionalised with ferrocene are ubiquitous.[8-10] Studies of electroactive monolayers containing transition metal coordination complexes are less common but include studies on Ru(II),[11-13] Os(II)[14] and Cu(II)[15] complex-functionalised monolayers. Ferrocene is commonly employed as a redox centre because it has a well-behaved redox potential (*ca.* +0.4 V *vs.* SCE) which is compatible with thiol SAM stability. There are drawbacks however; ferrocene derivatives can be poorly soluble and their redox processes are in fact relatively slow.[16] In contrast, ruthenium polypyridyl complexes can have significantly faster electron transfer processes in analogous alkanethiol monolayers on gold electrode surfaces.[17]

Although there is no doubt that ruthenium polypyridyl complexes with highly stable and well-understood coordination chemistry and long-lived excited state lifetimes (e.g. $Ru(bpy)_3^{2+}$) are desirable for a multitude of SAM-based applications, only limited studies on monolayers containing Ru(II) complexes have been undertaken. This is because, at the potentials of the Ru(II/III) polypyridyl redox process (*ca.* +1.1-1.2 V *vs.* SCE), oxidative desorption occurs so as to render the thiol-gold monolayers unstable.[19] SAMs of sulfur-containing adsorbates on gold have been shown to be electrochemically stable only within a limited potential window from -0.8 to +0.4 V_{MSE} (-0.4 to +0.8 V_{SCE}).[20]

For real-world applications thin film stability is essential, for example ruthenium-based dyes in dye-sensitized solar cells are expected to function for a number of years and to survive redox cycling without degradation. In order to achieve highly stable redox-active Ru(II) polypyridyl SAMs on gold surfaces, two separate strategies can be employed. Firstly the Ru(II/III) potential can be decreased so as to have a more easily accessible redox process and secondly, improvements to the stability of the

monolayer can be undertaken, e.g. by incorporating a more robust linker to the gold surface which is more stable than conventional thiol adsorbates.

The electrochemical and spectroscopic properties of Ru(II) complexes incorporating 2,2'-bipyridine (bpy) and 2,2':6',2"-terpyridine (tpy) ligands can be modified by introducing electron-withdrawing or -donating substituents onto the polypyridyl ligands.[21,22] Electron-releasing substituent groups such as pyrrolidine dramatically shift the ^{1}MLCT (metal to ligand charge transfer) absorption in the visible region, leading to more efficient visible light absorption coupled with a shift of the Ru(II/III) redox couple to less positive potentials.[22] In our case, we adopt this strategy incorporating a piperazine moiety at the 4' position of a terpyridine ligand which is coordinated to a Ru(II) or Os(II) metal centre.

In addition to improve the complex binding to the gold electrode surface, we present here the replacement of a thiol linker by the more robust dithiocarbamate (DTC) group. Wei *et. al.* have shown that dithiocarbamates adsorb strongly onto gold nanoparticles and can be prepared by simply combining a secondary amine with CS_2 in the presence of a gold surface.[23] Subsequent studies have demonstrated the versatility and robustness of this system.[24] Molecules with carbodithioate ($-CS_2^-$) groups are expected to have superior chemisorption properties over thiolates as their interatomic S-S distances are nearly ideal for adsorption onto Au surfaces.[25]

In this way the incorporaton of a piperazine group onto a tpy ligand serves the dual purpose of tuning the spectroscopic and electrochemical properties of the metal complexes, and provides a secondary amine site by which the complexes can be anchored to the gold surface (*via in situ* dithiocarbamate formation). Combining a reduced Ru(II/III) redox potential with the strength of the DTC linker allowed us to access stable redox-active monolayers on a gold surface functionalised with Ru(II) polypyridyl complexes for the first time.

Experimental Section

Reagents. Chemicals were purchased from Aldrich Chemical Co. Ltd. and were used without further purification. 4'-chloro-2,2':6',2"-terpyridine (Cltpy)[27] and 4'-phenyl-2,2':6',2"-terpyridine (phtpy)[28] were

prepared according to literature methods. Electrospray mass spectra were recorded on a micromass LCT electrospray mass spectrometer. Accurate mass spectra were referenced against Leucine Enkephalin (555.6 $g.mol^{-1}$) and reported within 5 ppm. Nuclear magnetic resonance spectra were recorded in deuterated acetonitrile with a Bruker Avance DPX-400 MHz at the following frequencies: 400.1 MHz for ^{1}H and 100.6 MHz for ^{13}C. Coupling constants were recorded in hertz (Hz) to two decimal places.

Electrochemistry. All electrochemical experiments were performed with a CH Instruments potentiostat model 660B. Cyclic voltammograms were measured on 1 mM solutions of the complexes in acetonitrile with tetra-*n*-butylammonium hexafluorophosphate ($TBAPF_6$, 0.1 M) as supporting electrolyte with a glassy carbon working electrode, a Pt wire counter electrode and a SCE as the reference electrode. Potentials are quoted *vs.* the ferrocene-ferrocenium couple (0.0 V), and all potentials were referenced to internal ferrocene added at the end of each experiment. The self-assembled monolayers were measured with the same setup and under the same conditions.

Monolayer Formation. Before immersing the 2 mm diameter gold electrodes into the solution of the complex, the surface was treated with piranha solution (70% conc. H_2SO_4 + 30% H_2O_2), rinsed with deionized water and polished with alumina (0.05 μm). After the polishing the electrode was thoroughly rinsed with water and methanol and the electrodes were again immersed into piranha solution. The chemical cleaning of the surface was followed by an electrochemical treatment of the gold electrode in H_2SO_4 (25 scans between 0 and 1.5 V vs Ag/AgCl-reference electrode at 0.05 Vs^{-1}). The freshly prepared gold electrode was immersed overnight into a 15 mM solution of the complex in 2:1 DMF:CS_2. The electrode was removed from the solution and washed thoroughly with acetone and acetonitrile to remove non-bound material.

[Ruthenium(II)(4'-phenyl-2,2':6',2"-terpyridine)(4'-chloro-2,2':6',2"-terpyridine)]$(PF_6)_2$ (3)

Ru(phtpy)Cl_3 (**1**): phtpy (0.97 mmol, 300 mg) and $RuCl_3.3H_2O$ (1.07 mmol, 277 mg) were heated together in 20 mL EtOH during 3 h. The reaction mixture was cooled and the resulting solid was

removed *via* filtration and washed well with water, ethanol and diethyl ether. The brown solid, 486 mg (0.942 mmol, 97%), was used without further purification.

Ru(phtpy)Cl_3 (0.387 mmol, 200 mg) and Cltpy (0.406 mmol, 109 mg) were combined in 10 mL ethylene glycol with 5 drops of N-ethylmorpholine and the suspension was heated at 70 °C for 3.5 h under N_2. A saturated aqueous solution of KPF_6 was added to the cooled reaction mixture to afford a red precipitate which was filtered over Celite and washed with water and diethyl ether. The crude product was purified *via* column chromatography (silica, CH_3CN:H_2O:sat. aq. KNO_3 = 20:3:1). The fractions containing the product were concentrated *in vacuo* and a saturated aqueous solution of KPF_6 was added to afford **3** as a red solid, 187 mg (0.193 mmol, 50%). ^{1}H NMR (CD_3CN): δ 9.00 (s, 2H), 8.86 (s, 2H), 8.64 (d, *J* = 8.03 Hz, 2H), 8.50 (d, *J* = 8.03 Hz, 2H), 8.21 (d, *J* = 7.53 Hz, 2H), 7.96 (m, 2H), 7.78 (dd, *J* = 7.53 Hz, 7.53 Hz, 2H), 7.70 (t, *J* = 7.53 Hz, 1H), 7.46 (d, *J* = 5.52 Hz, 2H), 7.39 (d, *J* = 5.52 Hz, 2H), 7.21 (m, 4H). ES-MS: Ru-isotopic pattern centered at *m/z* = 339.0427 (100%) $[M - 2PF_6]^{2+}$, calcd: 339.0436.

[Osmium(II)(4'-phenyl-2,2':6',2"-terpyridine)(4'-chloro-2,2':6',2"-terpyridine)]$(PF_6)_2$ (4)

Os(phtpy)Cl_3 (**2**): phtpy (0.46 mmol, 141 mg) and $(NH_4)_2[OsCl_6]$ (0.46 mmol, 200 mg) were heated together at 130 °C in 8 mL ethylene glycol during 3 h. The reaction mixture was cooled and the resulting solid was removed *via* filtration and washed well with water and diethyl ether. The black solid, 263 mg (0.43 mmol, 95%), was used without further purification.

Os(phtpy)Cl_3 (0.248 mmol, 150 mg) and Cltpy (0.248 mmol, 66 mg) were combined in 20 mL ethylene glycol with 5 drops of N-ethylmorpholine and the suspension was heated at 120 °C overnight under N_2. A saturated aqueous solution of KPF_6 was added to the cooled reaction mixture to afford a black precipitate which was filtered over Celite and washed with water and diethyl ether. The crude product was purified *via* column chromatography on a long column (silica, CH_3CN:H_2O:saturated aqueous KNO_3 = 20:3:1). The fractions containing the product were concentrated *in vacuo* and a saturated aqueous solution of KPF_6 was added to afford **4** as a black solid, 135 mg (0.128 mmol, 52%). ^{1}H NMR (CD_3CN): δ 9.06 (s, 2H), 8.90 (s, 2H), 8.64 (d, *J* = 8.03 Hz, 2H), 8.50 (d, *J* = 8.03 Hz, 2H),

8.20 (d, *J* = 7.60 Hz, 2H), 7.83 (m, 4H), 7.80 (dd, *J* = 7.60 Hz, 7.60 Hz, 2H), 7.65 (t, *J* = 7.60 Hz, 1H), 7.36 (d, *J* = 5.52 Hz, 2H), 7.26 (d, *J* = 5.52 Hz, 2H), 7.14 (m, 4H). ES-MS: Os-isotopic pattern centered at *m/z* = 384.0705 (100%) $[M - 2PF_6]^{2+}$, calcd: 384.0722.

[Ruthenium(II)(4'-phenyl-2,2':6',2"-terpyridine)(4'-(*N*-piperazinyl)-2,2':6',2"-terpyridine)]$(PF_6)_2$ (5)

$[Ru(phtpy)(Cltpy)](PF_6)_2$ (0.103 mmol, 100 mg) and piperazine (1.030 mmol, 89 mg) were dissolved in 40 mL CH_3CN and heated at reflux under N_2 for 20 h. The solution was reduced in volume and a saturated aqueous solution of KPF_6 was added to afford a dark red precipitate. The solid was removed *via* filtration over celite and washed well with water and diethyl ether. The dried solid was removed from the celite by redissolving in acetonitrile then evaporating to dryness *in vacuo* to afford red solid **5**, 104 mg (0.103 mmol, 100%). ^{1}H NMR (CD_3CN): δ 9.00 (s, 2 H), 8.66 (d, *J* = 8.03 Hz, 2 H), 8.49 (d, *J* = 8.03 Hz, 2 H), 8.22 (d, *J* = 7.53 Hz, 2H), 8.15 (s, 2 H), 7.96 (ddd, *J* = 8.03 Hz, 7.53 Hz, 1.50 Hz, 2 H), 7.89 (ddd, *J* = 8.03 Hz, 7.53 Hz, 1.50 Hz, 2 H), 7.78 (dd, *J* = 7.53 Hz, *J* = 7.53 Hz, 2 H), 7.69 (t, *J* = 7.53 Hz, 1 H), 7.54 (d, *J* = 5.52 Hz, 2 H), 7.34 (d, *J* = 5.52 Hz, 2 H), 7.26 (ddd, *J* = 7.53 Hz, 5.52 Hz, 1.50 Hz, 2 H), 7.10 (ddd, *J* = 7.53 Hz, 5.52 Hz, 1.50 Hz, 2 H), 3.82 (t, *J* = 5.02 Hz, 4 H), 3.13 (t, *J* = 5.02 Hz, 4 H); ^{13}C NMR (CD_3CN): δ 159.8, 159.5, 157.2, 157.0, 155.3, 153.5, 153.1, 147.9, 138.6, 138.5, 138.0, 131.1, 130.5, 128.6, 128.3, 127.8, 125.1, 124.7, 122.4, 108.9, 49.1, 46.4. ES-MS: Ru-isotopic pattern centered at *m/z* = 364.0975 (100%) $[M - 2PF_6]^{2+}$, calcd: 364.0975.

[Osmium(II)(4'-phenyl-2,2':6',2"-terpyridine)(4'-(*N*-piperazinyl)-2,2':6',2"-terpyridine)]$(PF_6)_2$ (6)

Synthesized using the same procedure as **5**, starting from $[Os(phtpy)(Cltpy)](PF_6)_2$ (0.095 mmol, 100 mg) and piperazine (0.946 mmol, 81 mg). **6** was isolated as a black solid, 104 mg (0.095 mmol, 100%). ^{1}H NMR (CD_3CN): δ 9.01 (s, 2H), 8.64 (d, *J* = 8.03 Hz, 2H), 8.48 (d, *J* = 8.03 Hz, 2H), 8.29 (s, 2H), 8.19 (d, *J* = 7.53 Hz, 2H), 7.83 (ddd, *J* = 8.03 Hz, 7.53 Hz, 1.50 Hz, 2H), 7.78 (m, 4H), 7.62 (t, *J* = 7.53 Hz, 1H), 7.38 (d, *J* = 5.52 Hz, 2H), 7.23 (d, *J* = 5.52 Hz, 2H), 7.19 (ddd, *J* = 7.53 Hz, 5.52 Hz, 1.50 Hz, 2H), 7.05 (ddd, *J* = 7.53 Hz, 5.53 Hz, 1.50 Hz, 2H), 4.19 (t, *J* = 5.02 Hz, 4H), 3.57 (t, *J* = 5.02 Hz, 4H); ^{13}C NMR (CD_3CN): δ 160.6, 160.4, 156.3, 156.2, 154.3, 152.2, 152.1, 145.5, 137.2, 137.15, 137.1,

130.0, 129.3, 127.9, 127.6, 127.2, 124.1, 124.0, 119.9, 106.5, 48.1, 45.5. ES-MS: Os-isotopic pattern centered at *m/z* = 409.1344 (100%) $[M - 2PF_6]^{2+}$, calcd: 409.1261.

Results and Discussion

Synthesis. Ruthenium and osmium complexes (**5** and **6**) functionalized with 4'-(*N*-piperazinyl)-2,2':6',2"-terpyridine (pztpy) and 4'-phenyl-2,2':6',2"-terpyridine (phtpy) were synthesized by reacting a ten-fold excess of piperazine with complexes **3** and **4** which contain both phtpy and 4'-chloro-2,2':6',2"-terpyridine (Cltpy) ligands (Scheme 1). Coordination of Cltpy to the metal centre activates the 4' position on the terpyridine ligand toward nucleophilic substitution,[29] thus the piperazinyl moiety replaces the chloro substituent to generate $[M(phtpy)(pztpy)](PF_6)_2$ in quantitative yield, without the need for the metal-catalyzed coupling typically required for the amination of heteroaryl halides.[30] The starting complexes **3** and **4** are prepared by firstly coordinating the phtpy ligand to the metal centre by reaction with either $RuCl_3.3H_2O$ or $(NH_4)_2[OsCl_6]$ to form $M(phtpy)Cl_3$ (**1** and **2** for Ru(III) and Os(III) respectively). Cltpy is then coordinated to the metal centres by heating the ligand together with $M(phtpy)Cl_3$ in ethylene glycol under nitrogen and in the presence of a reducing agent (N-ethylmorpholine) to form $[M(phtpy)(Cltpy)](PF_6)_2$ after column chromatography.

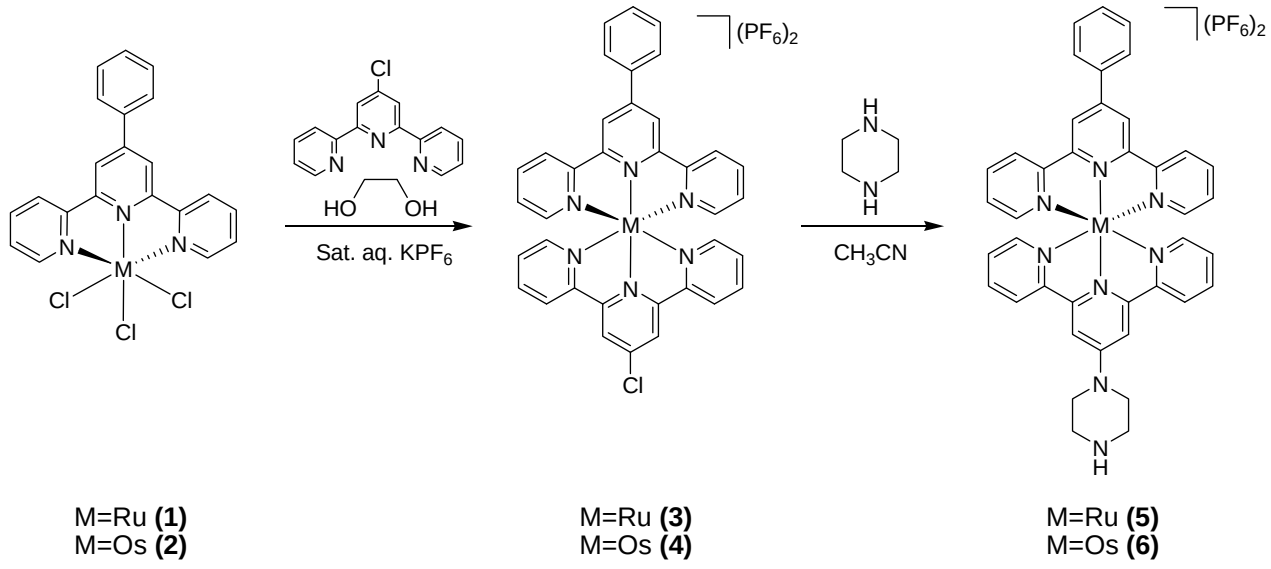

Scheme 1: The synthesis of Ru(II) and Os(II) complexes **5** and **6**.

The novel osmium and ruthenium complexes **5** and **6** have been characterized by NMR and UV-Vis spectroscopy, mass spectrometry and cyclic voltammetry. The aromatic ^{1}H NMR signals have been assigned with the aid of ^{1}H-^{1}H correlation spectroscopy experiments. The proton shifts are remarkably similar for both complexes; signals for the terpyridine system with piperazine at the 4' position (pztpy) are shifted upfield relative to the phenyl-substituted terpyridine, due to the electron-donating effect of the attached nitrogen from the piperazine ring (see supporting information).

Solution Spectroscopy. The UV-Vis absorption spectra of **5** and **6** (Figure 1) are dominated by strong MLCT transitions centered at λ_{max} 498 nm and λ_{max} 497 nm respectively and are quite similar, except for the presence of the formally spin-forbidden MLCT bands above 600 nm for the osmium complex. The MLCT absorptions are red-shifted by 23 nm from those of the unsubstituted bis-terpyridine complexes ($[Ru(terpy)_2]^{2+}$; λ_{max} = 475nm, $[Os(terpy)_2]^{2+}$; λ_{max} = 474nm).[31] This strong shift is a result of the electron donating effect of the nitrogen from the piperazinyl group bound to the terpyridine ligand. A similar effect has been observed for pyrrole- and pyrrolidine-substituted oligopyridine complexes[21,22] and can be attributed to the capacity of an electron-donor substituent to destabilize the HOMO metal orbital (π t_{2g}) more than the LUMO (π^*) ligand orbital.[32]

Error! Not a valid link.

Figure 1: UV-visible absorption spectra of Ru **5** (black line) and Os **6** (red line) complexes recorded in CH_3CN at room temperature.

Solution Electrochemistry. Both Ru **5** and Os **6** are electrochemically active and in both cases cyclic voltammetry in solution showed a single oxidation peak corresponding to the M(II/III) redox process. The cyclic voltammograms for solutions of **5** and **6** are shown in Figure 2. For **5** the reversible Ru(II/III) redox process was found to occur at +0.62 V (*vs.* Fc/Fc^+). This is at a significantly less positive potential than the unsubstituted parent complex $[Ru(tpy)_2]^{2+}$ which is oxidized at +0.92 V (*vs.* Fc/Fc^+).[31] The phenyl substituent has a minor effect on the position of the redox potential; two phtpy ligands result in the oxidation of $[Ru(phtpy)_2](PF_6)_2$ occurring at +0.90 V.[31-33] The major source of the decrease in the redox potential of **5** is the presence of the piperazine group on the pztpy ligand. The lone pair from the

nitrogen atom which is attached to the tpy can effectively conjugate with the π system of the tpy ligand. This results in increased electron density on the metal centre and as a result the Ru(II)→Ru(III) oxidation becomes a more accessible process. This observation is concurrent with the trend seen for other metal polypyridine complexes which have amine groups such as pyrrole or pyrrolidine attached[21,22] and is also in agreement with the red-shift of the MLCT observed in the absorption spectrum. The Ru(II/III) redox peak appears along with a broad shoulder which can only be seen on the oxidation wave of the voltammogram (Figure 2(a)). This feature is assigned to the oxidation of the pendent piperazine ring on the pztpy ligand. Piperazine itself was found to undergo an irreversible oxidation at +0.36 V *vs.* Fc/Fc^+. A similar broad shoulder has been noted in the literature for $[Ru(Xtpy)_2](PF_6)_2$ where X = pyrrole[21] and in a recent publication where X = 4-methylthiophenyl.[34]

Error! Not a valid link.Error! Not a valid link.

(a) (b)

Figure 2: Solution cyclic voltammograms of Ru **5** (a) and Os **6** (b) *vs.* Fc/Fc^+ in CH_3CN (1 mM) with 0.1 M $TBAPF_6$ as supporting electrolyte. Recorded at room temperature using a glassy carbon working electrode, a Pt wire counter electrode and a SCE reference electrode.

6 exhibits a reversible Os(II/III) redox process at +0.35 V (*vs.* Fc/Fc^+) in solution (Figure 2(b)) which is at a considerably less positive potential than that of the unsubstituted $[Os(tpy)_2](PF_6)_2$ (+0.58 V). Unlike the ruthenium equivalent, the CV for **6** is symmetrical and the broad peak due to the irreversible oxidation of the piperazinyl moiety cannot be seen. Since the Os(II) centre is more easily oxidized than the Ru(II) centre, oxidation of the piperazine group is therefore more difficult on the resulting Os(III) complex and can be observed as a broad oxidation with an onset at ca. 0.8V *vs*. Fc/Fc^+ on the CV (see supporting information).

Three reversible reductions which can be considered as ligand centered are observed for **5** (Figure 3) and like the Ru(II/III) oxidation peak, the positions of the ligand reductions are also shifted from $[Ru(tpy)_2](PF_6)_2$. The increased electron density on the tpy ligands due to the phenyl and piperazine substituents results in a cathodic shift as reduction of the pztpy and phtpy ligands is more difficult than that of unsubstituted tpy. We can assume that the first ligand reduction occurs on the phtpy ligand since

it will be the most easily reduced tpy ligand, while the pztpy ligand should be relatively more difficult to reduce as a result of the added electron density resulting from the piperazine substituent. For osmium complex **6** the reduction processes were poorly resolved on the cyclic voltammogram. A summary of the peak potentials measured for complexes **5** and **6** is presented in Table 1 along with comparative data for $[Ru(tpy)_2](PF_6)_2$ and $[Os(tpy)_2](PF_6)_2$.

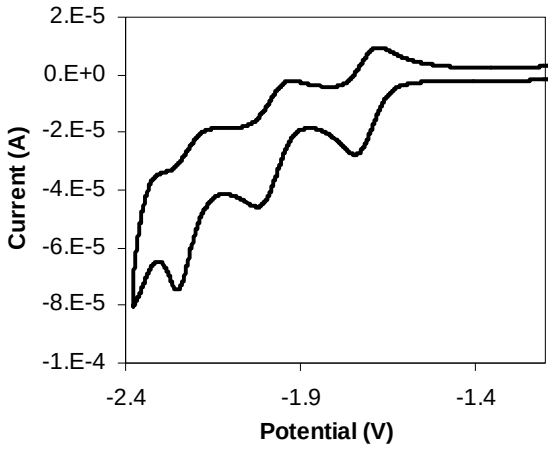

Figure 3: Cyclic voltammogram of **5** showing the ligand-based reduction peaks *vs.* Fc/Fc^+ in CH_3CN (1 mM) with 0.1 M $TBAPF_6$ as supporting electrolyte. Recorded at room temperature using a glassy carbon working electrode, a Pt wire counter electrode and a SCE reference electrode.

Table 1: Oxidation and reduction processes for **5** and **6** as compared to the unsubstituted $[M(tpy)_2](PF_6)_2$ complexes.

	M^{II} - M^{III} (V)[a]	Reductions (V)[a]		
Ru (**5**)	0.62	-1.71	-1.98	-2.21
$[Ru(tpy)_2](PF_6)_2$[b]	0.92	-1.67	-1.92	
Os (**6**)	0.35	*c*		
$[Os(tpy)_2](PF_6)_2$[b]	0.58	-1.63	-1.95	

[a] In CH_3CN solution (1 mM) with 0.1 M $[NBu^n_4][PF_6]$ as supporting electrolyte, measured *vs.* internal ferrocene/ferrocenium. [b] Reference [31]. [c] Reductive processes poorly resolved.

Preparation of Self-Assembled Monolayers. Complexes **5** and **6** were used to form self-assembled monolayers on gold electrodes *via* the *in situ* formation of a DTC anchoring group at the piperazinyl nitrogen on the pztpy ligand (Scheme 2). The gold electrodes used were carefully polished and electrochemically cleaned before SAM formation was attempted by immersing the electrodes overnight into mixtures of the appropriate complex and CS_2 in DMF as described in the experimental section. The resulting SAMs were characterized by cyclic voltammetry in acetonitrile with $[NBu^n_4][PF_6]$ as supporting electrolyte.

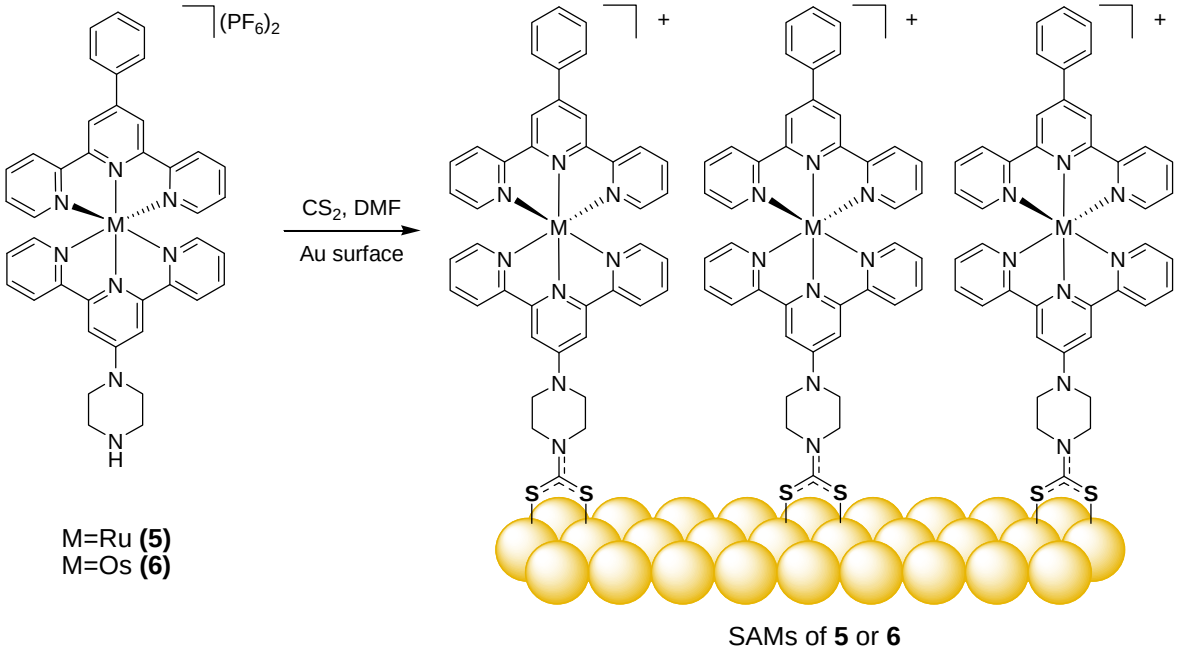

Scheme 2: The formation of DTC-anchored SAMs of complexes **5** and **6** on gold surfaces.

Electrochemical Response of Self-Assembled Monolayers. Typical cyclic voltammograms obtained for SAMs of **5** and **6** are plotted in Figure 4. The CVs show the typical Gaussian shape of redox active surface-bound species. The redox peaks for both complexes are symmetrical and the broad shoulder which can be seen in the solution CV of the ruthenium complex is no longer present. This is further evidence that the shoulder observed in Figure 2(a) is due to the oxidation of the pendent amine on the

piperazine ring of **5**. When the complex is attached to the gold electrode surface the amine group has been converted to a dithiocarbamate functionality and hence its oxidation cannot occur. The characteristic values observed for both complexes such as half potentials (E^0_{surf}), surface coverage (Γ_s) and the full-width-at-half-maximum (FWHM) are listed in Table 2.

Error! Not a valid link.

Figure 4: Cyclic voltammograms showing the M^{II}-M^{III} processes for SAMs of **5** (black line) and **6** (red line) *vs.* Fc/Fc^+. Recorded at room temperature at a scan rate of 8 Vs^{-1} in CH_3CN with 0.1 M $[NBu^n_4][PF_6]$ as supporting electrolyte, using a Pt wire counter electrode and a SCE reference electrode.

Table 2: Electrochemical properties of SAMs of **5** and **6** adsorbed onto gold electrodes with a DTC anchoring group, measured in acetonitrile with 0.1 M $[NBu^n_4][PF_6]$ as supporting electrolyte. All potentials refer to the Fc/Fc^+ redox couple.

	E^0_{sol} (V)	E^0_{surf} (V)	$FWHM_{surf}$(V)	Γ_s (mol cm^{-2})
Ru (**5**)	0.62	0.61	0.15	$5.8x10^{-11}$
Os (**6**)	0.35	0.35	0.12	$5.1x10^{-11}$

The peak potentials of the surface-bound complexes (E^0_{surf}) remain effectively unshifted from the solution species (E^0_{sol}), indicating that the terminal nitrogen on the pendent piperazinyl ring (now converted to a DTC group) does not greatly influence the environment at the metal centre. This is expected since the methylene carbon units of the piperazine ring would not induce efficient electron delocalization between the terminal nitrogen and the rest of the molecule. The peak split for Ru **5** and Os **6** at small scan rates is below 50 mV indicating sufficient electron transfer rates under such conditions. The FWHM of the redox peaks is around 150 mV indicating relatively strong repulsive interactions as has been discussed extensively for this type of complex on platinum surfaces.[35] The saturation surface coverages (Γ_s) were calculated from the charge under the oxidation and reduction

peaks of the cyclic voltammograms (Ru **5**: 5.8×10^{-11} mol cm^{-2} and Os **6**: 5.1×10^{-11} mol cm^{-2}). The surface coverages of the complexes are found to be greater than those observed for related bis-terpyridine compounds, e.g. $[M(tpy)(pytpy)](PF_6)_2$ (pytpy = 4'-(4-pyridyl)-2,2':6',2"-terpyridine) which form SAMs on Pt surfaces *via* the pendent pyridyl nitrogen, provide surface coverages of 2.5×10^{-11} mol cm^{-2} for M=Ru and 3.3×10^{-11} mol cm^{-2} for M=Os.[36] The increased surface concentration for SAMs of **5** and **6** on gold electrodes will be heavily influenced by the strong affinity of the DTC group for gold. Other factors such as different intermolecular interactions (repulsive or attractive) between surface-bound species will also affect the surface coverage.

CVs were run at increasing scan rates for SAMs of **5** and **6**. Typical surface behavior was reflected in the linear dependence of the peak current as a function of scan rate, and is illustrated for the peak current of the anodic signal of Ru **5** in Figure 5. It can be concluded that complexes bound to gold surfaces by the DTC group form ideal self-assembled monolayers comparable to complexes bound to Au electrodes via thiol groups or to platinum by pyridine functionalities.

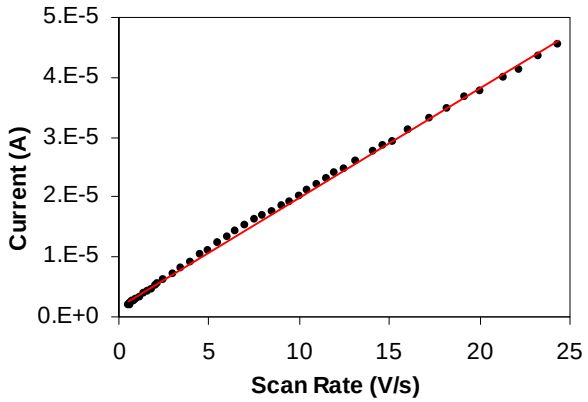

Figure 5: Peak current as a function of scan rate for SAMs of **5**.

Assembling data collected from successive scans at increased scan rates allows for an estimation of the rate constant of the electrochemical reaction (k) and also the charge transfer coefficient (α) using Laviron's methodology.[37] The heterogeneous rate constant measures the intrinsic ability of an oxidized species to exchange electrons with the electrode in order to convert to its reduced form, and *vice versa*.

A species with a large value of *k* will convert to its redox partner rapidly. The transfer coefficient ($0 < \alpha < 1$) is indicative of the symmetry of the energy barrier for a redox half-reaction. In an ideal reversible reaction, the energy required to convert the reduced species into its oxidized equivalent is equal to the energy required to reverse the process such that $\alpha = 0.5$. Deviation from the ideal value of 0.5 is indicative of an asymmetrical relationship between the oxidized and reduced forms of a compound.

Using Laviron's method, data were examined where the difference between the anodic and cathodic peak potentials (ΔE_p) is greater than 200/n mV (n being the number of electrons transferred in the redox reaction). Plots of the anodic (E_{pa}) and cathodic (E_{pc}) peak positions against ln *v* (scan rate) yielded straight lines with slopes corresponding to $-RT/(1-\alpha)nF$ and $-RT/\alpha nF$ for the anodic and cathodic plots respectively. Appling Laviron's methodology to data obtained from successive scans of complexes **5** and **6** results in typical Laviron plots as shown in Figure 6.

Error! Not a valid link.Error! Not a valid link.

(a) (b)

Figure 6: Laviron plots of the anodic and cathodic peak positions for Ru **5** (a) and Os **6** (b) from CVs recorded in CH_3CN *vs*. SCE. Linear plots are taken from where $\Delta E_p > 200$ mV.

E_p E_p

For **5** the transfer coefficient α is found to be 0.54 as calculated from the slopes of the linear plots ($\Delta E_p > 200$ mV) in Figure 6 (a). The heterogeneous rate constant for the Ru(II/III) redox reaction in SAMs of **5** was found to be approximately 351 s^{-1}. For osmium complex **6,** α is found to be 0.55 while *k* is found to be 248 s^{-1}. The values calculated for the charge transfer coefficients for the Ru(II/III) and Os(II/III) reactions are close to the ideal value of 0.5 and are indicative of a high degree of reversibility in the redox transformation for both complexes. This would suggest that oxidation and reduction of the surface-bound species is a relatively stable process and providing that the link to the surface is sufficiently robust, monolayers of **5** and **6** should endure a large number of cycles without degradation.

The rate constants (*k*) obtained using the Laviron calculations are not particularly fast, as was expected given the observed scan-rate dependence of the peak positions. There are very few examples of Ru(II) and Os(II) polypyridyl complexes incorporated into SAMs, but one recent publication

describes a Ru(II) bis-tpy complex with two pendent octanethiolate arms which is used to form SAMs on gold electrodes and nanoparticles.[38] The Ru(II/III) electron transfer rate constant was calculated using Laviron's methodology and assuming that $\alpha = 0.5$, k was found to be ~3.5 s^{-1}. The rate constant was found to increase significantly to 11.5 s^{-1} when the distance between the redox centre and the electrode surface was shortened. Electron-transfer rate constants have been obtained for SAMs of other metal polypyridyl complexes but these are too dissimilar from the bis-tpy complexes presented here to draw a direct comparison.[17,39] The values of 351 s^{-1} and 248 s^{-1} calculated for **5** and **6** suggest that the electron transfer rates for SAMs of the complexes are faster than those of other bis-tpy thiol-based complexes.

Stability of the SAMs. Having already demonstrated the favourable shift in potential of the new Ru(II) and Os(II) polypyridine complexes, our aim was to quantify the electrochemical stability of the resulting SAMs. This was achieved experimentally by systematically expanding the potential window of the cyclic voltammetry experiment and examining the charge under the redox peaks to observe the effect of applying greater voltages to the SAM. 100 cycles were run on the electrode between 0 and +0.5 V (*vs*. Fc/Fc^+) and the charge under the Ru(II/III) oxidation peak was measured. Subsequent sets of 100 scans were run with the potential window of the CV being systematically expanded by 0.1 V each time. The area under the oxidation peak was measured after each set of scans and the results of this experiment are plotted in Figure 7.

Error! Not a valid link.

Figure 7: The faradaic charge under the anodic peak as a function of the upper potential applied to SAMs of **5** (100 scans applied at each interval).

Up to a potential of about +1 V *vs.* $Fc\text{-}Fc^+$, the charge under the redox signal (and by extension, the surface coverage of the SAM) remains constant and it can be concluded that the SAM of the complex is stable up to this potential. Still at +1.1 V only less than 10 % of the faradaic charge is lost. Since at each potential 100 cycles were run, at +1.1 V the system had endured 700 voltammetric cycles. Clearly the SAMs are indeed very robust and the dithiocarbamate-gold binding is very strong. Other sulfur

adsorbates such as thiols are only known to be stable up to approximately +0.4 V *vs.* $Fc\text{-}Fc^{+}$.[20] The DTC linker offers a significant improvement over the conventional thiol group. This is highly relevant to current research since a large number of ruthenium oligopyridine complexes with interesting electrochemical and photochemical properties have potentials around 1 V; the dithiocarbamate anchoring group could enable surface-bound electrochemical investigation of such complexes.

To further test the stability of the monolayers, electrodes modified with the SAMs were immersed into 12 mM solutions of 2-mercaptoethanol (ME) in methanol. A control was set up in which the modified electrode was immersed into methanol so that the effect of ME could be determined. 2-mercaptoethanol is used to rapidly strip thiol monolayers from gold surfaces *via* an exchange reaction and typically after 24 h the original thiol monolayer is completely removed from the gold surface.[23,40] The charge under the M(II/III) redox peak was measured in order to estimate the number of molecules attached to the electrode surface.

For Ru(II) complex **5**, after 24 h there was a 31% reduction in the charge under the redox peak for the SAMs exposed to ME. For SAMs stored in MeOH a reduction of 21% was observed. After 48 h and then 6 days, the CVs showed little change, however the redox peaks for the monolayer exposed to the ME solution broadened. This could to be due to the 2-mercaptoethanol units attaching to the gold surface along with the adsorbed complexes of **5**, but since the Ru(II/III) redox peak is still observable it would seem that the thiol is unable to displace the dithiocarbamate-bound monolayer.

For Os(II) complex **6**, after 24 h the SAMs exposed to ME were depleted by just 3% while SAMs kept in methanol were depleted by 6%. After 48 h there was further depletion in the redox peaks but after 6 days there was very little difference between the two samples; a 23% decrease in the charge under the redox peak for the SAM exposed to ME and 20% decrease for the SAM stored in MeOH. The results do exhibit some variation but essentially they demonstrate that 2-mercaptoethanol does not strip the DTC-anchored SAMs in the same manner as it does for thiol-based SAMs. Detecting the SAMs at 80% of their original intensity after storing for 6 days in methanolic solutions of ME is convincing evidence of their robustness.

Conclusions

There is much incentive for the design of robust, well-ordered SAMs displaying tethered polyimine complexes, in particular a wide range of Ru(II) complexes would be worthy subjects for the formation of ordered electro-active nanostructures. The light harvesting and fast electron-transfer properties of such complexes could then be exploited in device applications that favour monolayer construction, e.g. solar cells or organic light emitting diodes, in addition to the development of responsive electrochemical sensors. Until now the attachment of such polyimine complexes to gold surfaces in useful devices has been hindered by two separate problems. The first involves the demandingly high redox potentials of the majority of Ru(II) polypyridyl complexes. The second is the poor chemical and electrochemical stability of the universally-employed thiol tethers. This investigation overcomes these problems by incorporating a piperazine group onto a polypyridine ligand attached to a metal complex. This modification makes more efficient the resulting complexes' optical and electronic properties: notably causing a red shift of the ^{1}MLCT and a concomitant cathodic shift of the redox potential. Furthermore the same group provides a site for robust dithiocarbamate attachment of the complex to a gold surface. Synthetically the construction of the pztpy ligand on complexes **5** and **6** was quantitative and no further purification was required.

A DTC-anchoring group was readily employed to generate SAMs of **5** and **6** from the *in situ* reaction of the piperazine (as a secondary amine) with CS_2 in the presence of a gold substrate. The strong bidentate attachment of the DTC linker to gold surface atoms is a result of a near ideal interatomic S-S distance. Electrochemical investigation of SAMs of **5** and **6** revealed their ideal surface behavior. Data obtained from successive CVs at increasing scan rates allowed calculation of charge transfer coefficients that were close to the ideal value of 0.5 and electron transfer rate constants that were faster than SAMs of comparable compounds. The surface coverage of the SAMs proved to be significantly larger than that reported for SAMs of other bis-tpy complexes in the literature. Crucially the DTC SAMs were found to be exceptionally robust, resisting potentials and stripping agents which are known to destroy thiol-based SAMs on gold surfaces.

In summary, the SAMs of complexes **5** and **6** present a significant improvement over any related systems in the literature. The combination of the exceptional DTC anchoring group and the tuned photo- and electrochemical properties of the metal complexes has allowed us to produce what must be considered as the most stable Os(II) and in particular Ru(II) bis-terpyridine complex SAMs to date. This unique and versatile approach to constructing ordered assemblies of metal complexes on gold surfaces offers exciting possibilities for the application of a range of useful Ru(II) complexes in the form of robust functional self-assembled monolayers.

Acknowledgements

SFI-05PICA and E.I.-travel award for funding to F.M. and E.F. Dr. John O'Brien for NMR spectroscopic measurements.

Supporting Information Available

^{1}H NMR spectra of complexes **5** and **6**, CV of **6** showing piperazine oxidation.

Pictorial Table of Contents

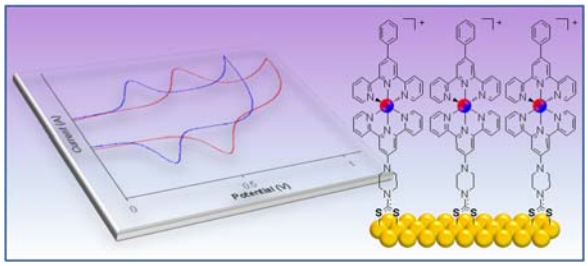

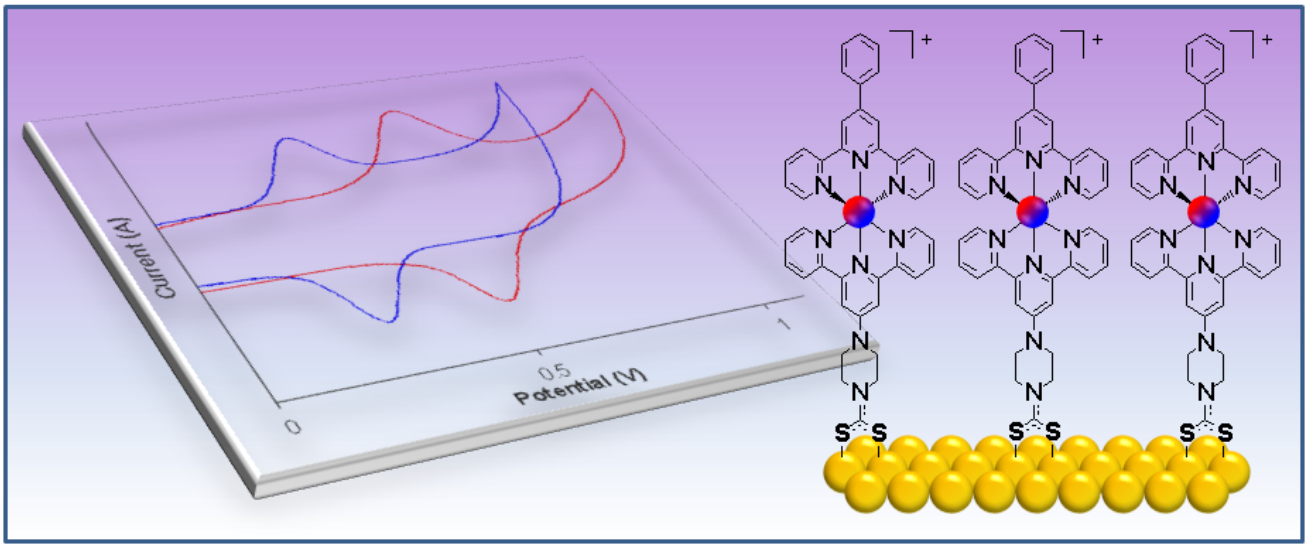

(1) Hickmann, J. J.; Ofer, D.; Laibinis, P. E.; Whitesides, G. M.; Wrighton, M. S. *Science* **1991**, *252*, 688-691.

(2) Chaki, N. K.; Vijayamohanan, K. *Biosensors & Bioelectronics* **2002**, *17*, 1-12.

(3) Devillers, C. H.; Boturyn, D.; Bucher, C.; Dumy, P.; Labbé, P.; Moutet, J.-C.; Royal, G.; Saint-Aman, E. *Langmuir* **2006**, *22*, 8134 -8143.

(4) Baron, R.; Onopriyenko, A.; Katz, E.; Lioubashevski, O.; Willner, I.; Wang, S.; Tian, H. *Chemical Communications* **2006** 2147-2149.

(5) Péter, M.; Li, X.-M.; Huskens, J.; Reinhoudt, D. N. *Journal of the American Chemical Society* **2004**, *126*, 11684-11690.

(6) Ravenscourt, M. S.; Finklea, H. O. *Journal of Physical Chemistry* **1994**, *98*, 3843-3850.

(7) Smalley, J. F.; Sachs, S. B.; Chidsey, C. E. D.; Dudek, S. P.; Sikes, H. D.; Creager, S. E.; Yu, C. J.; Feldberg, S. W.; Newton, M. D. *Journal of the American Chemical Society* **2004**, *126*, 14620-14630.

(8) Chidsey, C. E. D. *Science* **1991**, *251*, 919-922.

(9) Smalley, J. F.; Feldberg, S. W.; Chidsey, C. E. D.; Linford, M. R.; Newton, M. D.; Lid, Y.-P. *Journal of Physical Chemistry* **1995**, *99*, 13141-13149.

(10) Weber, K.; Hockett, L.; Creager, S. *J. Phys. Chem. B* **1997**, *101*, 8286-8291.

(11) Smalley, J. F.; Finklea, H. O.; Chidsey, C. E. D.; Linford, M. R.; Creager, S. E.; Ferraris, J. P.; Chalfant, K.; Zawodzinsk, T.; Feldberg, S. W.; Newton, M. D. *Journal of the American Chemical Society* **2003**, *125*, 2004-2013.

(12) Eberspacher, T. A.; Collman, J. P.; Chidsey, C. E. D.; Donohue, D. L.; Van Ryswyk, H. *Langmuir* **2003**, *19*, 3814-3821.

(13) Haga, M. a.; Hong, H. G.; Shiozawa, Y.; Kawata, Y.; Monjushiro, H.; Fukuo, T.; Arakawa, R. *Inorganic Chemistry* **2000**, *39*, 4566-4573.

(14) Haddox, R. M.; Finklea, H. O. *J. Phys. Chem. B* **2004**, *108*, 1694-1700.

(15) Freire, R. S.; Kubota, L. T. *The Analyst* **2002**, *127*, 1502-1506.

(16) Patoux, C.; Coudret, C.; Launay, J.-P.; Joachim, C.; Gourdon, A. *Inorganic Chemistry* **1997**, *36*, 5037-5049.

(17) Hortholary, C.; Minc, F.; Coudret, C.; Bonvoisin, J.; Launay, J.-P. *Chemical Communications* **2002**, 1932-1933.

(18) Vos, J. G.; Kelly, J. M. *Dalton Transactions* **2006**, 4869-4883.

(19) Finklea, H. O. *Electroanalytical Chemistry*; Marcel Dekker: New York, 1996; Vol. 19.

(20) Beulen, M. W. J.; Kastenberg, M. I.; Veggel, F. C. J. M. v.; Reinhoudt, D. N. *Langmuir* **1998**, *14*, 7463-7467.

(21) Martineau, D.; Gros, P.; Beley, M.; Fort, Y. *Eur. J. Inorg. Chem.* **2004**, 3984-3986.
(22) Martineau, D.; Beley, m.; Gros, P. C. *Journal of Organic Chemistry* **2006**, *71*, 566-571.
(23) Zhao, Y.; Perez-Segarra, W.; Shi, Q.; Wei, A. *Journal of the American Chemical Society* **2005**, *127*, 7328-7329.
(24) Vickers, M. S.; Cookson, J.; Beer, P. D.; Bishop, P. T.; Thiebaut, B. *J. Mater. Chem.* **2006**, *16*, 209-215.
(25) Colorado, R.; Villazana, R. J.; Lee, T. R. *Langmuir* **1998**, *14*, 6337-6340.
(26) Alves, C. A.; Smith, E. L.; Porter, M. D. *J. Am. Chem. Soc.* **1992**, *114*, 1222-1227.
(27) Constable, E. C.; Ward, M. D. *Journal of the Chemical Society, Dalton Transactions* **1990**, 1405-1409.
(28) Wang, J.; Hanan, G. S. *Synlett* **2005**, 1252-1254.
(29) Constable, E. C. *Chemical Society Reviews* **2007**, *36*, 246-253.
(30) Johansson, O. *Synthesis* **2006**, *15*, 2585-2589.
(31) Constable, E. C.; Thompson, A. M. W. C. *Journal of the Chemical Society, Dalton Transactions* **1994**, 1409-1418.
(32) Maestri, M.; Armaroli, N.; Balzani, V.; Constable, E. C.; Thompson, A. M. W. C. *Inorganic Chemistry* **1995**, *34*, 2759-2767.
(33) Constable, E. C.; Cargill Thompson, A. M. W.; Tocher, D. A.; Daniels, M. A. M. *New Journal of Chemistry* **1992**, *16*, 855-867.
(34) Constable, E. C.; Housecroft, C. E.; Medlycott, E.; Neuburger, M.; Reinders, F.; Reymann, S.; Schaffner, S. *Inorganic Chemistry Communications* **2008**, *11*, 518-520.
(35) Figgemeier, E.; Constable, E. C.; Housecroft, C. E.; Zimmermann, Y. C. *Langmuir* **2004**, *20*, 9242-9248.
(36) Figgemeier, E.; Merz, L.; Hermann, B. A.; Zimmermann, Y. C.; Housecroft, C. E.; Guntherodt, H. J.; Constable, E. C. *J. Phys. Chem. B* **2003**, *107*, 1157-1162.
(37) Laviron, E. *Journal of Electroanalytical Chemistry* **1979**, *101*, 19-28.
(38) Dong, T.-Y.; Huang, C.; Chen, C.-P.; Lin, M.-C. *Journal of Organometallic Chemistry* **2007**, *692*, 5147-5155.
(39) Ricci, A.; Rolli, C.; Rothacher, S.; Baraldo, L.; Bonazzola, C.; Calvo, E.; Tognalli, N.; Fainstein, A. *Journal of Solid State Electrochemistry* **2007**, *11*, 1511-1520.
(40) Demers, L. M.; Mirkin, C. A.; Mucic, R. C.; Reynolds, R. A.; Letsinger, R. L.; Elghanian, R.; Viswanadham, G. *Anal. Chem.* **2000**, *72*, 5535-5541.

Supporting Information

Robust SAMs of Ru(II) and Os(II) Polypyridines on Gold Surfaces: Exploring New Potentials

Frances A. Murphy[a], Stèphane Suarez[a], Egbert Figgemeier[b], Emma R. Schofield[a], Sylvia M. Draper[a,*]

[a] *Chemistry Department, Sami Nasr Institute of Advanced Materials (SNIAM), Trinity College Dublin, College Green, Dublin 2, Ireland.*

[b] *Department of Chemistry, University of Basel, Spitalstrasse 51, 4056 Basel, Switzerland.*

NMR Characterisation of 5 and 6:

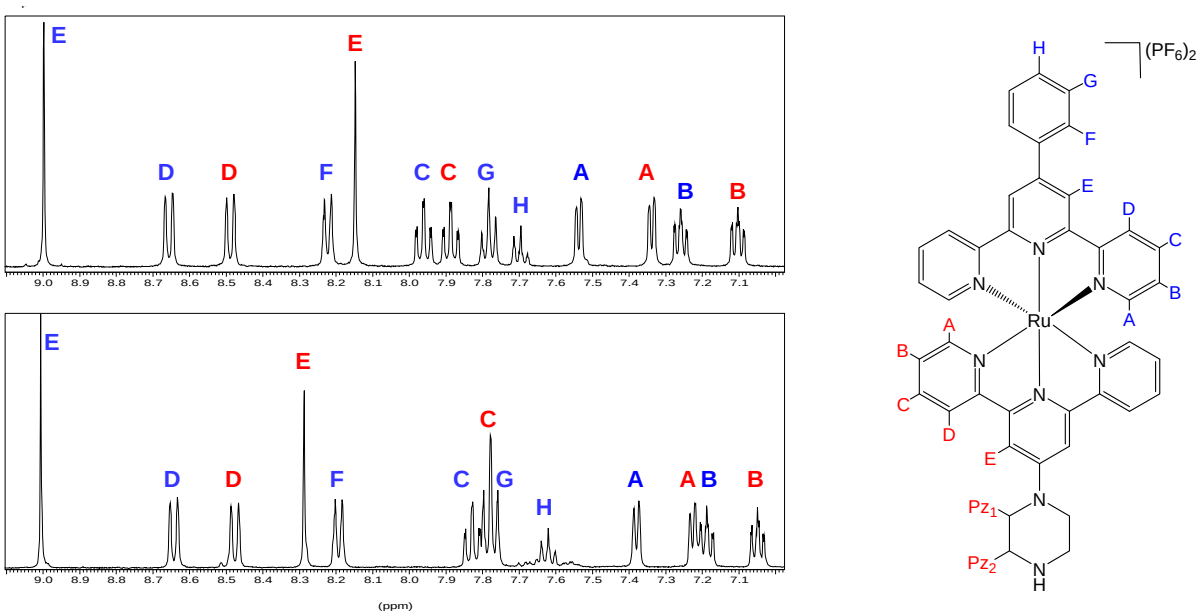

Figure 2: ^{1}H NMR spectra for Ru 5 (top) and Os 6 (bottom). Recorded in CD_3CN at 400.1 MHz.

Chart 1: ^{1}H NMR chemical shifts (ppm) for Ru **5** and Os **6**.

Proton	A	B	C	D	E	F	G	H	A	B	C	D	E
5	7.54	7.26	7.96	8.66	9.00	8.22	7.78	7.69	7.34	7.10	7.89	8.49	8.15
6	7.38	7.19	7.83	8.64	9.01	8.19	7.78	7.62	7.23	7.05	7.78	8.48	8.29

Solution Cyclic Voltammetry of 6:

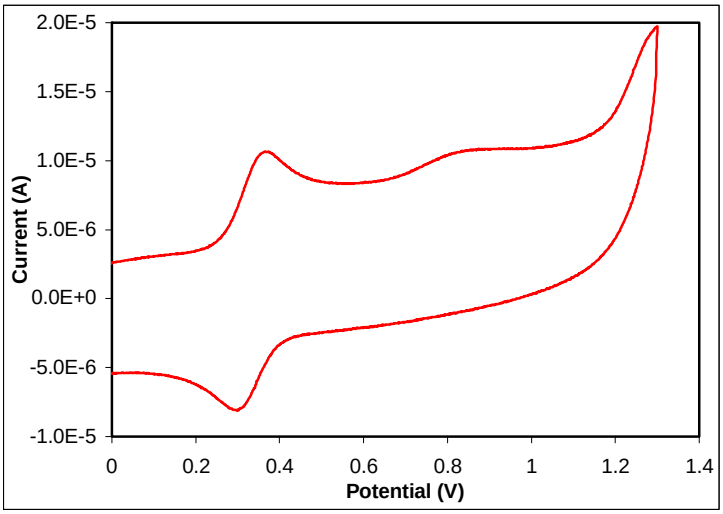

Figure 3: Solution cyclic voltammogram of Os **6** *vs.* Fc/Fc^{+} in CH_3CN (1 mM) with 0.1 M $TBAPF_6$ as supporting electrolyte, showing the irreversible piperazine oxidation at *ca.* +0.8 V. Recorded at room temperature using a glassy carbon working electrode, a Pt wire counter electrode and a SCE reference electrode.

Stability of SAMs of 5 and 6:

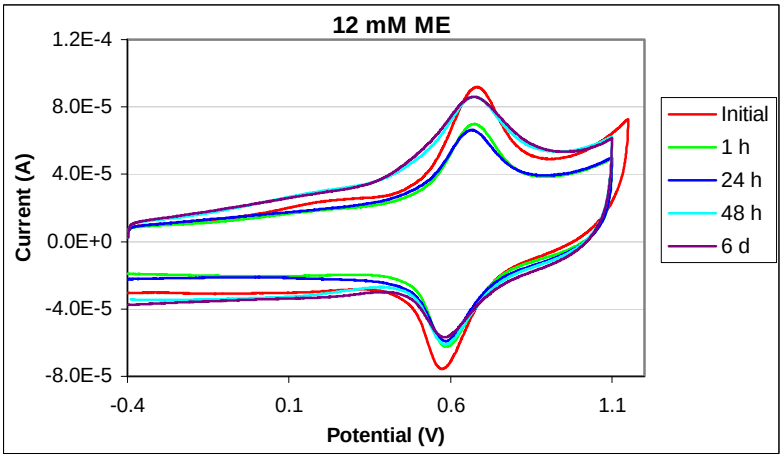

Figure 4: Cyclic voltammogram of a SAM of **5** when exposed to 12 mM 2-mercaptoethanol in methanol.

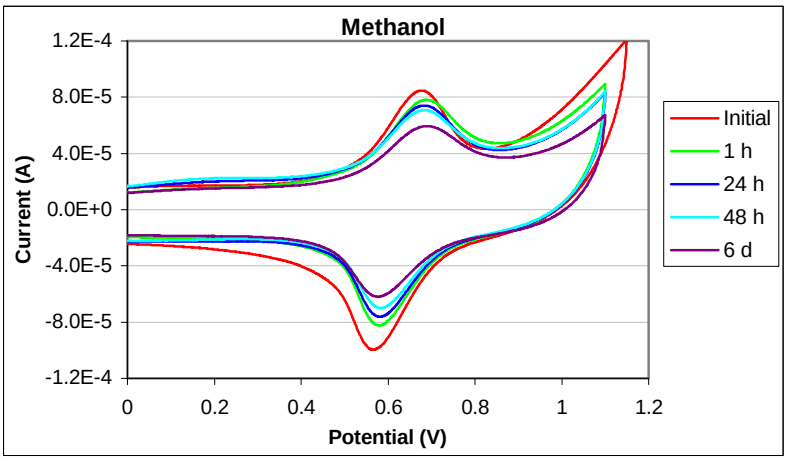

Figure 5: Cyclic voltammogram of a SAM of **5** when immersed in methanol.

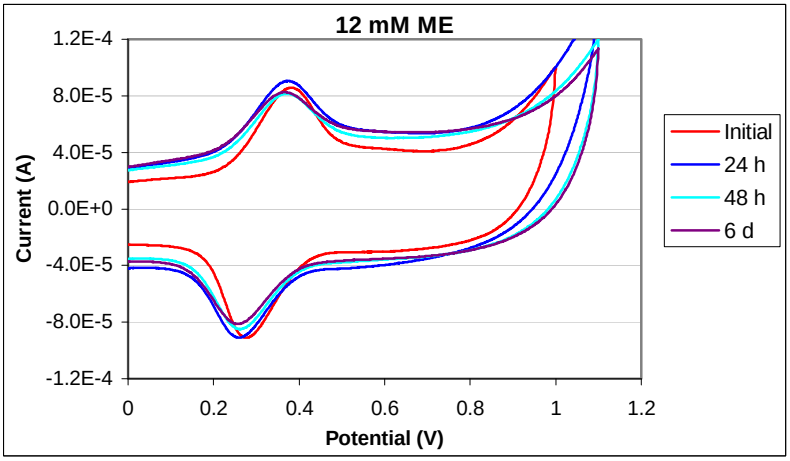

Figure 6: Cyclic voltammogram of a SAM of **6** when exposed to 12 mM 2-mercaptoethanol in methanol.

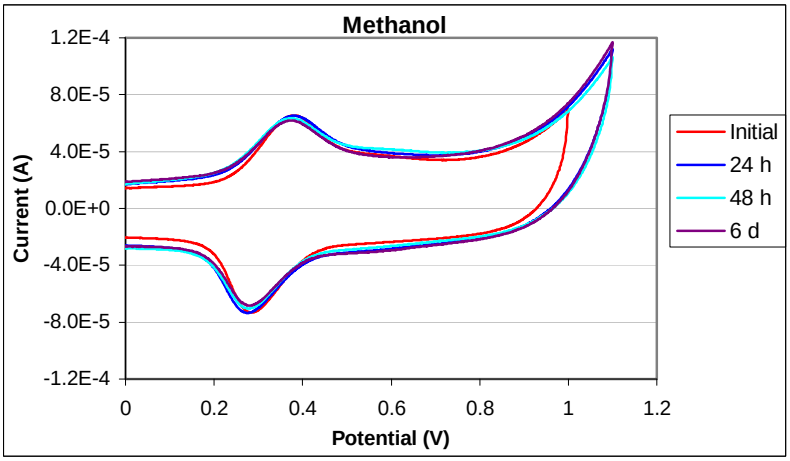

Figure 7: Cyclic voltammogram of a SAM of **6** when immersed in methanol.